Light Through the Geometric Memory of Spacetime

Optical Signatures in Gravitational Lensing

Alejandro Rey
Independent Researcher, Argentina
reyalejandro311@gmail.com

July 16, 2026

Abstract

Gravitational lensing does not measure matter directly. A light ray follows the optical geometry encoded in the metric, and any mass distribution is inferred only afterward from the curvature required to explain its path. This paper develops that observation into a weak-field constitutive hypothesis: the optical geometry sampled by light may contain delayed curvature, left by a gravitational response that relaxes toward the baryonic configuration with a finite time, described by the minimal closure $\tau_{\mathrm{eff}}\mathcal{L}_u q + q = q_{\mathrm{eq}}$. In relaxed systems the residual is nearly stationary; in young, merging, tidally perturbed, or rapidly reorganized systems the same residual can appear as optical excess or spatial lag. The primary test is weak lensing. The residual template is fixed outside the lensing sample by the SPARC/RAR scale; the same scale defines the reference clock $\tau_{\mathrm{vac}} = 36.6\,\mathrm{Myr}$. The leading quadrupolar optical closure then predicts $A_{\mathrm{rel}} = 19/15 = 1.2667$, without fitting the lensing amplitude. When the KiDS profile is projected onto the same fixed template it returns $A_{\mathrm{rel}} = 1.267 \pm 0.032$, while an independent HSC holdout is consistent within 0.84σ. Population splits show the predicted ordering: redder and more centrally concentrated lenses require a larger optical projection than blue or low-Sérsic lenses. Strong-lensing SLACS systems and eleven gold double-radio relic mergers are treated as supporting checks of the same physical picture: structural optical excess and temporal phase lag. These results support a concrete reading: light may be curving through residual weak-field geometry, not only through an instantaneous mass distribution.

1 The observable is the path of light

A photon crossing a galaxy or a merging cluster does not carry a label telling us which component of the stress-energy tensor produced the curvature it encountered. It follows a null geodesic of the metric. The observer then solves the inverse problem: which optical geometry would have bent the ray that way? Only after that inversion do we translate the curvature into a lensing mass. The geometry sampled by a null congruence separates naturally into a Ricci component, associated with matter in the beam, and a Weyl shear component, associated with tidal fields outside the beam [12, 13].

This order matters. The observation itself is more primitive than the mass model: light has crossed an optical geometry stronger, or differently located, than the geometry expected from the instantaneous baryonic distribution. The question asked here is therefore not how to fit a halo first. The question is whether the optical geometry seen by light can contain memory.

The physical picture is simple. Matter moves, collides, forms stars, loses gas, and rearranges itself. Standard quasi-static weak-field reconstructions lock the optical geometry to the instantaneous visible source. If instead the weak-field response has a finite relaxation time, then the light ray may cross curvature that still remembers a recent source configuration. The mass interpretation comes later; the optical fact comes first.

This makes the best laboratories clear before any fit is performed. Memory should be most visible where the source has been driven out of equilibrium: cluster mergers, young or recently reorganized galaxies, systems under strong tidal forcing, and low-density environments where local relaxation is slow. The present paper focuses on lensing because it is the cleanest entrance to the idea. Lensing measures geometry directly.

1.1 What the photon samples

The relevant optical quantity is not a local density but an integral of the metric along the line of sight. In weak-field language, the deflection and convergence are controlled by the lensing potential, usually written as a combination of the scalar metric perturbations Φ and Ψ [2, 11, 13–15]. A photon therefore samples the geometry accumulated along its trajectory:

$$\alpha^i \propto \int \nabla_\perp^i (\Phi + \Psi)\, d\chi. \tag{1}$$

If the metric contains a residual component that is still relaxing, that component enters the same optical integral. The photon does not distinguish between instantaneous curvature and delayed curvature; it follows the total geometry.

This is the relativistic core of the proposal. The observable is the optical tidal field along a null congruence, before any mass reconstruction is introduced. A finite relaxation time leaves residual weak-field curvature along that path; a standard lensing reconstruction then translates the residual optical geometry into an effective mass distribution. Figure 1 summarizes this distinction.

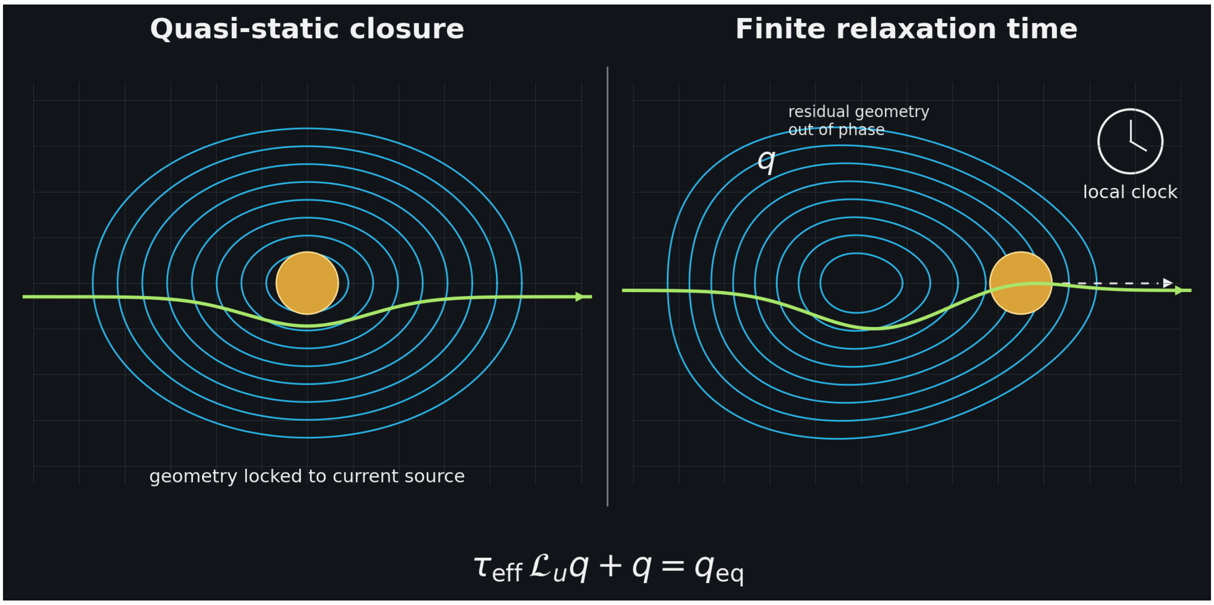

Figure 1: Conceptual schematic of the constitutive hypothesis. In the quasi-static closure, the optical geometry is reconstructed as locked to the current baryonic source. With finite relaxation time, residual weak-field geometry q remains out of phase with the moving or reorganized source. A light ray follows the total optical geometry, so delayed curvature can contribute to the inferred lensing mass.

2 The rheology of weak-field geometry

The previous section describes the observational side: light samples optical geometry along its path. The theoretical question is what kind of weak-field geometry the light is sampling. The usual quasi-static reconstruction treats the coarse-grained response as effectively elastic: the source configuration is specified and the field is reconstructed as if it adjusted without delay. The alternative studied here is rheological. Weak-field geometry is allowed to carry an internal polarization that relaxes toward the baryonic equilibrium over a finite local time. I refer to this constitutive weak-field framework below as TIDE. Related metric-affine analyses show how post-Riemannian tidal terms can enter geodesic deviation, providing a useful geometric template for organizing such residual tidal responses [17].

Let q denote the residual weak-field geometry that would ordinarily be reconstructed as an effective halo after subtracting the baryonic contribution. This definition is operational first: q names the part of the reconstructed weak-field response not accounted for by the instantaneous baryonic field. The theory then models that residual as a relaxing geometric polarization, not as a new substance or particle species. In the scalar, long-wavelength limit used below this means

$$q \equiv g_{\rm rec} - g_{\rm bar}, \tag{2}$$

where $g_{\rm rec}$ is the weak-field response reconstructed from the observable and $g_{\rm bar}$ is the instantaneous baryonic prediction. Here "coarse-grained" means averaged over the weak-field scale: the constitutive relation applies to the long-wavelength gravitational response, not to individual particle trajectories. The instantaneous closure assumes

$$q = q_{\rm eq}, \tag{3}$$

where $q_{\rm eq}$ is the relaxed residual selected by the baryonic configuration. The constitutive completion replaces this algebraic relation by a causal one-pole response:

$$\tau_{\rm eff}\mathcal{L}_u q + q = q_{\rm eq}. \tag{4}$$

Here $\mathcal{L}_u$ is the derivative along the local coarse-grained frame and $\tau_{\rm eff}$ is the relaxation time of the effective weak-field response.

Equation (4) is the central object. It is the minimal retarded closure for a weak-field residual with finite memory. In the limit $\tau_{\rm eff} \to 0$, the standard instantaneous closure is recovered. For finite $\tau_{\rm eff}$, the residual depends on recent source history.

Equivalently, the photon can outrun the relaxation of the coarse-grained geometry. A photon travels on the null cone of the metric, while the residual weak-field response relaxes over $\tau_{\rm eff}$. When the source configuration changes on a time shorter than the local relaxation time, light samples a geometry that is out of phase with the instantaneous baryonic distribution. This phase lag is the physical origin of the effective optical residual.

The construction keeps one physical metric for matter and light. No separate photon metric is introduced. Any optical excess must therefore come from how the same residual weak-field geometry contributes to the scalar potentials Φ and Ψ. The response is also causal: q cannot know the future source configuration, and in the absence of continued driving it relaxes toward $q_{\rm eq}$ over the local time $\tau_{\rm eff}$. The empirical question is therefore not only how much baryonic matter is present, but how much time the geometry has had to respond to it.

The one-pole law in Eq. (4) is the retarded constitutive limit of a dissipative EFT construction in which q is a coarse-grained response variable, following the logic of dissipative effective actions and gravitational EFT organization [5–7]. The present paper uses this leading limit because it is the part directly tested by lensing and lag observables. The complete non-linear optical closure belongs to the next order of the EFT expansion, rather than being an additional assumption needed for the weak-lensing projection check.

The reference value used in this work is fixed by the galactic weak-field scale,

$$\tau_{\rm vac} = \frac{V_*}{a_0} = 36.6\,{\rm Myr}, \tag{5}$$

where a_0 is the empirical radial-acceleration scale and V_* is the SPARC velocity scale measured from the 175-galaxy SPARC sample [9, 10]. This number is not chosen from the lensing data. It is the galactic benchmark obtained from the observed RAR/SPARC weak-field scale and then carried into the lensing calculation as a fixed reference. It is a benchmark, not a universal constant:

the effective clock can depend on environment, curvature and dynamical state. In the static weak-lensing audit, the diagnostic optical amplitude is evaluated against the externally fixed RAR residual template and the geometric projection 19/15, not by an independent variation of τ_{eff}. The reference clock sets the temporal interpretation of the constitutive response and the scale for genuinely time-dependent lag tests.

3 Memory-induced optical slip

The residual q is calibrated dynamically: it is the extra weak-field response needed to organize massive tracers. Lensing asks how the same residual enters the optical metric. In a weak-field scalar notation,

$$ds^2 = -(1 + 2\Psi)dt^2 + a^2(t)(1 - 2\Phi)d\mathbf{x}^2, \tag{6}$$

massive tracers respond primarily to Ψ, while lensing responds to the Weyl combination $(\Phi + \Psi)/2$. A residual that organizes dynamics need not project into light with unit amplitude. The leading quadrupolar metric response gives a definite optical projection,

$$\Phi_{\text{opt,q}} = A_{\text{rel}}\, \Psi_q, \tag{7}$$

with

$$A_{\text{rel}}^{\text{geom}} = 1 + \alpha_{\text{W}} = 1 + \frac{4}{15} = \frac{19}{15} = 1.2667. \tag{8}$$

Here $A_{\text{rel}} = 1$ would mean that the scalar dynamical closure already gives the full optical amplitude. The factor 4/15 is the leading STF/quadrupolar projection factor of the residual tidal response into the optical metric: it is the smallest tensor correction beyond the scalar dynamical floor.

In this sense A_{rel} is the weak-field trace of a memory-induced optical slip within a single metric. The residual geometry contributes differently to the dynamical potential and to the Weyl potential that bends light. In the relaxed, purely scalar limit one expects $A_{\text{rel}} \simeq 1$. In a nonlinear or tidally activated regime, where the residual carries anisotropic geometric information, the optical projection can exceed the scalar dynamical projection.

This is the quantity the data can test. If q were merely a dynamical bookkeeping device, lensing would not have to see it coherently. If q is residual geometry, light must respond to it through the optical metric. The geometric value in Eq. (8) therefore turns the weak-lensing fit into a zero-refit optical check: does light see the predicted projection of the residual that organizes dynamics?

The constitutive picture therefore predicts that the optical excess should carry visible structural information rather than act as a blind constant applied to every lens. Temporal lag is most exposed in systems driven out of equilibrium, but optical projection is a different question: red, spheroidal, high-Sérsic lenses can carry a stronger accumulated tidal/Weyl component than blue, low-Sérsic systems. The population prediction tested below is structural ordering, not a universal monotonic rule with compactness alone.

4 Weak lensing: testing the optical projection

The primary quantitative test uses galaxy-galaxy weak lensing [4]. Operationally, the observable is the excess surface-density profile $\Delta\Sigma(R)$: the mean tangential distortion of background galaxies around an isolated lens. We compare that profile with the instantaneous baryonic prediction and ask whether the residual weak-field template projects coherently into the optical metric.

The scalar residual template is not learned from the lensing data. It is fixed before looking at the lensing amplitude by the same SPARC/RAR weak-field scale used to define the reference clock. The optical amplitude is also fixed here, using the geometric value $A_{\text{rel}} = 19/15$ from Eq. (8). This is therefore not a test of whether the RAR can be reproduced once more. The weak-lensing question is different and relativistic: does light read that externally fixed residual with the predicted optical projection?

For isolated KiDS lenses the full-covariance projection onto the fixed template returns

$$A_{\mathrm{rel}} = 1.267 \pm 0.032. \tag{9}$$

This data-space reconstruction differs from the geometric prediction 19/15 by only 0.023σ, with $\Delta\chi^2 = 5.2 \times 10^{-4}$ relative to the best free-amplitude reconstruction. In the combined GAMA+KiDS block-diagonal check the fixed geometric value lies within 0.21σ of the best-fit amplitude. An independent HSC S16A holdout [1], with 9826 lenses, returns a diagnostic $A_{\mathrm{rel}} = 1.348 \pm 0.090$, consistent with 19/15 within 0.84σ; with the KiDS value held fixed the HSC profile gives $\chi^2/N = 0.71$, while baryons-only gives $\chi^2/N = 75.4$. The result is therefore not only an optical excess above the scalar dynamical closure; it is an optical excess landing on the leading geometric projection.

The sharper test is not only where the global projection lands, but its ordering across lens populations. The splits are pre-specified by visible lens properties, not by the lensing signal itself. They give

Split	Lower-response bin		Higher-response bin	
	Population	A_{rel}	Population	A_{rel}
Colour	blue	0.865 ± 0.053	red	1.555 ± 0.048
Sérsic index	low-n	0.945 ± 0.053	high-n	1.470 ± 0.049

The differences are large: 9.7σ for red–blue and 7.3σ for high–low Sérsic. This is the important point for the physical narrative. The lensing residual tracks visible structure rather than acting as an arbitrary constant, as expected if light is crossing residual geometry tied to the baryonic configuration and its relaxation state.

Parsimony relative to standard halo modeling

The point is not that standard halo modeling cannot fit these systems. It can, but not until a halo profile, concentration, stellar mass-to-light ratio, environment and line-of-sight contribution are specified. The relevant distinction is parsimony: the residual template is fixed outside the lensing sample, and the optical conversion is fixed by the quadrupolar value $A_{\mathrm{rel}} = 19/15$. The test asks whether that fixed value lands on the reconstructed optical response.

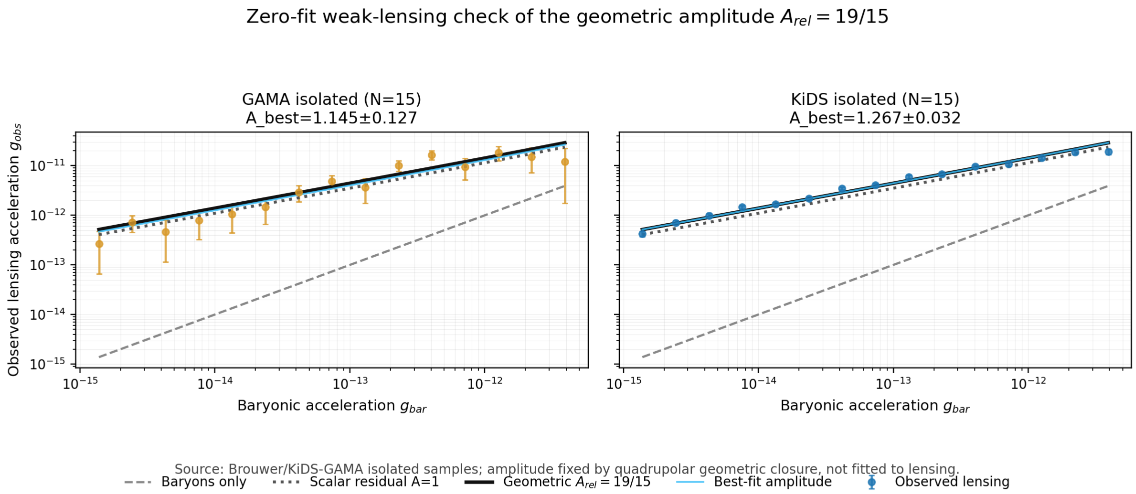

Figure 2: Zero-refit weak-lensing check of the geometric projection. The residual template is fixed outside the lensing samples and the optical projection is fixed to $A_{\rm rel} = 19/15$. In KiDS isolated lenses ($N = 15$ radial covariance bins), the geometric curve is essentially indistinguishable from the best free-amplitude reconstruction. GAMA isolated lenses are lower but consistent within 1σ. In both samples, baryons alone fail by a large margin.

The structural splits provide a second layer of information. They show that the optical excess is not a blind constant: red and high-Sérsic lenses require a larger projection than blue and low-n lenses, as expected if the photon is crossing residual geometry tied to baryonic structure and its relaxation history.

5 Strong lensing: the same question at higher optical depth

Strong lenses ask a higher-optical-depth version of the same question [16]. The Einstein radius is sensitive to the integrated projected geometry, line-of-sight structure, stellar population assumptions and baryonic profile modeling. The useful question here is structural: does the strong-lensing excess carry the same visible-compactness information expected from a geometric response?

In a 56-lens SLACS audit [3], the observed enhancement $\theta_E/\theta_{E,\rm bar}$ anticorrelates with stellar compactness:

$$\rho_{\rm S}(\log\Sigma_*, \theta_E/\theta_{E,\rm bar}) = -0.480, \qquad p = 1.825\times10^{-4}.$$

The parameter-free scalar TIDE/RAR mapping predicts the same sign and a very similar structural ordering,

$$\rho_{\rm S}(\log\Sigma_*, \theta_{E,\rm TIDE}/\theta_{E,\rm bar}) = -0.506, \qquad p = 6.826\times10^{-5}.$$

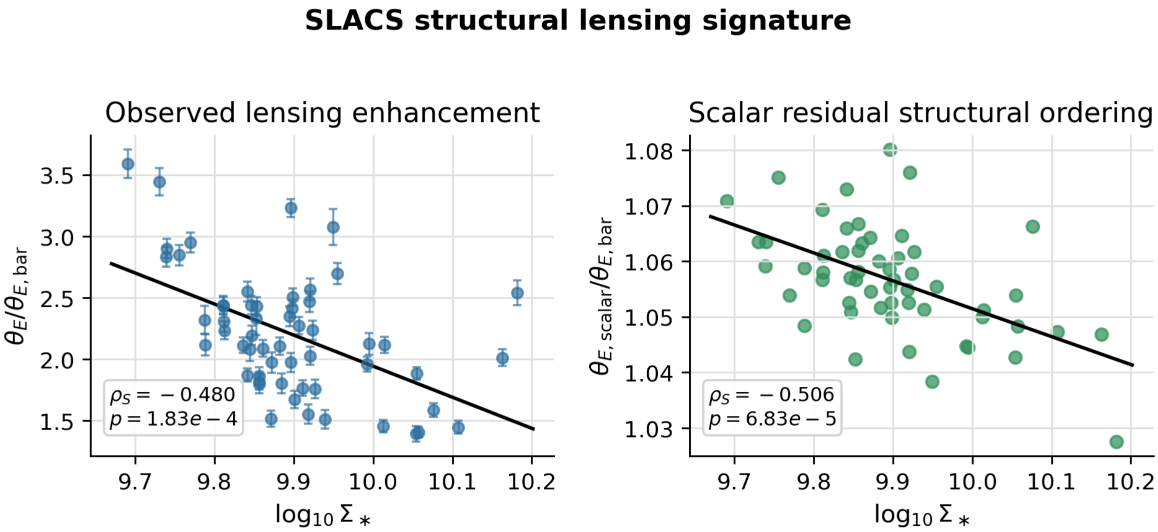

Figure 3: Strong-lensing structural check in SLACS ($N = 56$ lenses). The observed lensing enhancement anticorrelates with stellar compactness, and the scalar residual mapping gives the same sign of structural ordering before any lens-by-lens halo tuning. This figure is used as a structural consistency check, not as a full strong-lensing likelihood.

The scalar map is used here only as a structural predictor. A full strong-lensing model must include the relativistic optical closure, line-of-sight structure and detailed baryonic modeling. The relevant point for the present paper is narrower: the direction of the structural dependence appears before any lens-by-lens halo tuning.

The two lensing results are consistent with a single physical picture. Weak lensing gives the clean projection test: the leading geometric value $A_{\rm rel} = 19/15$ lands on the KiDS reconstruction and survives an HSC holdout. Strong lensing then asks whether the same residual carries visible structure at higher optical depth. It does. The scalar residual remains the leading floor of the optical geometry crossed by light, not its full relativistic ceiling.

6 Merging clusters: when memory becomes spatial lag

The most intuitive place to look for delayed geometry is a violent merger. In a dissociative collision, gas shocks and slows, galaxies continue almost collisionlessly, and the reconstructed lensing geometry need not remain coincident with the shocked baryons. In the constitutive picture, this is the same memory seen in another projection: recent source history has become a spatial phase lag.

The cleanest current merger check uses the eleven gold double-radio-relic clusters of Ref. [8]. These systems provide a common observable: the radio shock separation $d_{\rm shock}$, the reconstructed lensing separation $d_{\rm halo}$, and a published time-since-collision estimate. The test is intentionally not the old same-definition gas–lensing offset test. It asks a different question: is the reconstructed lensing geometry systematically behind the shock phase?

In this sample the sign is uniform:

$$d_{\rm halo} < d_{\rm shock} \quad \text{in} \quad 11/11 \text{ systems},$$

with a one-sided binomial probability $p = 4.88 \times 10^{-4}$. Defining the half-gap

$$L_{\rm lag} = \frac{d_{\rm shock} - d_{\rm halo}}{2},$$

one also finds a correlation with the published time-since-collision:

$$r_{\rm Pearson} = 0.812, \quad p = 2.42 \times 10^{-3},$$

and

$$\rho_{\text{Spearman}} = 0.723, \quad p = 1.19 \times 10^{-2}.$$

A zero-intercept fit gives an effective phase speed

$$v_{\text{lag}} = 994 \pm 28\,\text{km}\,\text{s}^{-1}.$$

This speed is of the order of the characteristic infall speeds of dissociative cluster mergers. In the present interpretation it should not be read as a new universal clock, but as the projected phase speed at which the shock–lensing separation accumulates during the merger history.

This result should be compared directly with merger simulations in cold and self-interacting dark matter. Its relevance here is temporal: the reconstructed lensing geometry is not coincident with the radio shock phase, and the lag grows with the published collision clock. It is therefore used here as a supporting temporal check, not as a stand-alone discriminator between dark-sector models.

7 Conclusion

The tests assembled here read the same physical object from different angles: the optical geometry crossed by light. Weak lensing is the central test. The residual template is fixed outside the lensing sample and the leading quadrupolar optical closure predicts $A_{\text{rel}} = 19/15 = 1.2667$. Projecting the isolated KiDS profile onto the same fixed template returns $A_{\text{rel}} = 1.267 \pm 0.032$, and an independent HSC holdout remains consistent. Population splits show that the excess is not a blind constant; it tracks baryonic structure in the predicted direction. This is the parsimonious part of the test: the data are not asked to build a halo, but to tell whether light projects a pre-defined residual geometry coherently.

The supporting checks point the same way without carrying the same statistical weight. Strong lensing shows the same structural sign in 56 SLACS systems. Radio relic mergers add the temporal dimension: in eleven gold systems, the reconstructed lensing separation lags the radio shock separation, and the lag grows with the published collision clock.

Taken together, the tests support a single optical statement:

> Light can be deflected by residual weak-field geometry whose relaxation is not instantaneous.

Only at this stage does the dark-halo language enter. If an observer reconstructs mass from delayed optical geometry, the result will look like an effective halo. The result is deliberately narrower than a replacement of the entire dark sector: a measurable part of halo phenomenology can be organized as delayed geometry with a finite relaxation time.

The minimal law $\tau_{\text{eff}}\mathcal{L}_u q + q = q_{\text{eq}}$ turns this picture into a testable framework. The next step is technical: extend the leading quadrupolar optical closure into a full relativistic lensing operator, test the environmental dependence of τ_{eff}, and implement the non-linear response in spatially resolved simulations. The evidence assembled here gives a concrete target for that work: the path of light appears to remember more geometry than the instantaneous baryonic field alone.

Data and Code Availability

The reproducibility archive contains the input tables, analysis scripts, provenance notes where available, generated figures and numerical outputs for the weak-lensing optical-projection check, the geometric 19/15 weak-lensing prediction check, the SLACS structural check and the radio-relic merger phase-lag test. The archive is deposited at Zenodo; DOI: `https://doi.org/10.5281/zenodo.21385597`.

Acknowledgements

The author thanks the open astronomical-data community and the developers of the public numerical tools used in the reproducibility package. This work was carried out independently, without institutional funding or dedicated computational allocation. AI-assisted tools were used for computational assistance, code auditing, editorial iteration and consistency checks; all scientific content, the central idea, methodological decisions and conclusions remain the sole responsibility of the author.

References

[1] Aihara, H., Arimoto, N., Armstrong, R., et al. 2018, PASJ, 70, S4.

[2] Bartelmann, M., & Schneider, P. 2001, Physics Reports, 340, 291.

[3] Bolton, A. S., Burles, S., Koopmans, L. V. E., Treu, T., & Moustakas, L. A. 2008, ApJ, 682, 964.

[4] Brouwer, M. M., Oman, K. A., Valentijn, E. A., et al. 2021, A&A, 650, A113. arXiv:2106.11677.

[5] Crossley, M., Glorioso, P., & Liu, H. 2017, JHEP, 09, 095. arXiv:1511.03646.

[6] Gubitosi, G., Piazza, F., & Vernizzi, F. 2013, JCAP, 02, 032. arXiv:1210.0201.

[7] Israel, W., & Stewart, J. M. 1979, Annals of Physics, 118, 341.

[8] Jee, M. J., Park, D., & Lee, W. 2026, arXiv:2605.00093.

[9] Lelli, F., McGaugh, S. S., & Schombert, J. M. 2016, AJ, 152, 157.

[10] McGaugh, S. S., Lelli, F., & Schombert, J. M. 2016, Physical Review Letters, 117, 201101.

[11] Narayan, R., & Bartelmann, M. 1996, arXiv:astro-ph/9606001.

[12] Jordan, P., Ehlers, J., & Sachs, R. K. 1961, Akademie der Wissenschaften und der Literatur Mainz, Abhandlungen der Mathematisch-Naturwissenschaftlichen Klasse, 1.

[13] Sachs, R. K. 1961, Proceedings of the Royal Society of London A, 264, 309.

[14] Seitz, S., Schneider, P., & Ehlers, J. 1994, Classical and Quantum Gravity, 11, 2345.

[15] Schneider, P., Ehlers, J., & Falco, E. E. 1992, *Gravitational Lenses* (Berlin: Springer).

[16] Treu, T. 2010, Annual Review of Astronomy and Astrophysics, 48, 87.

[17] van de Venn, A., Netz-Marzola, M., Vasak, D., & Struckmeier, J. 2026, arXiv:2606.27433.

A Technical clarifications

This appendix collects the technical conventions behind the main text. It is not an additional model layer; it only makes explicit what is meant by the residual field, the optical amplitude and the reference clock.

A.1 Operational meaning of q

The field q is defined operationally before it is modeled dynamically. In a weak-field reconstruction one first computes the response expected from the instantaneous baryonic distribution. The remaining reconstructed response is the residual:

$$q \equiv g_{\rm rec} - g_{\rm bar} \tag{10}$$

in the scalar, long-wavelength limit used here. The constitutive hypothesis then identifies this residual with a coarse-grained geometric polarization that relaxes toward a baryon-selected equilibrium,

$$\tau_{\rm eff}\mathcal{L}_u q + q = q_{\rm eq}. \tag{11}$$

Thus q is the reconstructed weak-field residual, interpreted as a retarded component of the geometry rather than as an independently assigned halo.

A.2 Why lensing can measure the residual

Massive tracers and photons project the metric differently. In the weak-field scalar notation used in the main text, non-relativistic tracers respond mainly to Ψ, while lensing responds to the optical combination $(\Phi + \Psi)/2$. If the residual is a genuine metric response rather than a bookkeeping device, it must enter this optical combination. At leading quadrupolar order, the scalar residual projects as

$$\Phi_{\rm opt,q} = A_{\rm rel}\,\Psi_q. \tag{12}$$

The minimal STF/quadrupolar projection gives

$$A_{\rm rel}^{\rm geom} = 1 + \frac{4}{15} = \frac{19}{15}. \tag{13}$$

The lensing reconstruction $A_{\rm rel} > 1$ should therefore be read as an optical response of the residual geometry. It is not a second metric for light; it is a statement about how the same weak-field residual contributes to the Weyl potential sampled by null geodesics.

A.3 Leading quadrupolar origin of 19/15

The numerical value used in the weak-lensing check is the leading quadrupolar projection of a tidal residual into the optical metric. Let Q_{ij} denote the symmetric trace-free angular quadrupole,

$$Q_{ij} = n_i n_j - \frac{1}{3}\delta_{ij}. \tag{14}$$

The isotropic angular average gives

$$\langle n_i n_j n_k n_l\rangle = \frac{1}{15}\left(\delta_{ij}\delta_{kl} + \delta_{ik}\delta_{jl} + \delta_{il}\delta_{jk}\right), \tag{15}$$

and therefore

$$\langle Q_{ij}Q_{kl}\rangle = \frac{2}{15}\mathcal{P}^{\rm STF}_{ijkl}, \qquad Q_{ij}Q^{ij} = \frac{2}{3}. \tag{16}$$

The normalized STF projection is thus 1/5. The trace-removal/Ward projection that maps the spatial tidal residual into the lensing potential contributes the factor 4/3. The leading optical correction is therefore

$$\alpha_{\mathrm{W}}^{\mathrm{geom}} = \frac{4}{3} \times \frac{1}{5} = \frac{4}{15}, \qquad A_{\mathrm{rel}}^{\mathrm{geom}} = 1 + \alpha_{\mathrm{W}}^{\mathrm{geom}} = \frac{19}{15}. \tag{17}$$

This is the value held fixed in the weak-lensing prediction. Higher-order tidal operators can change the strong-lensing regime, but they are not used in the leading weak-lensing amplitude check.

A.4 How the SPARC reference clock is obtained

The value $\tau_{\mathrm{vac}} = 36.6\,\mathrm{Myr}$ is not introduced by the lensing analysis. It is the reference clock associated with the SPARC/RAR weak-field scale. In the scalar constitutive limit, the relaxed residual is controlled by one acceleration scale a_0. Writing the characteristic flat-curve velocity of the SPARC sample as V_*, the constitutive identification is

$$a_0 = \frac{V_*}{\tau_{\mathrm{vac}}}, \qquad \tau_{\mathrm{vac}} = \frac{V_*}{a_0}. \tag{18}$$

Using $V_* \simeq 138.5\,\mathrm{km\,s^{-1}}$ for the 175-galaxy SPARC sample and $a_0 \simeq 1.2 \times 10^{-10}\,\mathrm{m\,s^{-2}}$ gives

$$\tau_{\mathrm{vac}} \simeq 1.15 \times 10^{15}\,\mathrm{s} \simeq 36.6\,\mathrm{Myr}. \tag{19}$$

Thus the number used in the main text is the SPARC/RAR reference time inferred from the galactic weak-field scale and then carried into the lensing analysis as an external benchmark. It is not treated as a universal constant. In the static weak-lensing check, the quantity held fixed is the RAR residual template selected by the same galactic scale, together with the leading geometric optical projection $A_{\mathrm{rel}} = 19/15$. The clock becomes directly observable in time-dependent systems, where a residual response can appear as a spatial phase lag accumulated over a finite relaxation time.

A.5 Leading-order closure and next-order terms

The paper uses the leading scalar closure. This is enough to define the residual template and test its optical projection, while leaving the full relativistic optical closure to the next stage. That next order is expected to contain tidal/Weyl operators, anisotropic stress and environmental dependence of τ_{eff}. In that language, the weak-lensing projection A_{rel} is the first optical projection of the residual, while the strong-lensing audit tests whether the same structural dependence appears in a higher-optical-depth regime. A full spatially resolved implementation is the natural next step.